bnhcrc.com.au

SECONDARY EYEWALL FORMATION IN TROPICAL CYCLONES

Peer reviewed research proceedings from the Bushfire and Natural Hazards CRC & AFAC conference
Sydney, 4 – 6 September 2017

Jeffrey D. Kepert
Bureau of Meteorology and Bushfire and Natural Hazards CRC

Corresponding author: Jeff.Kepert@bom.gov.au

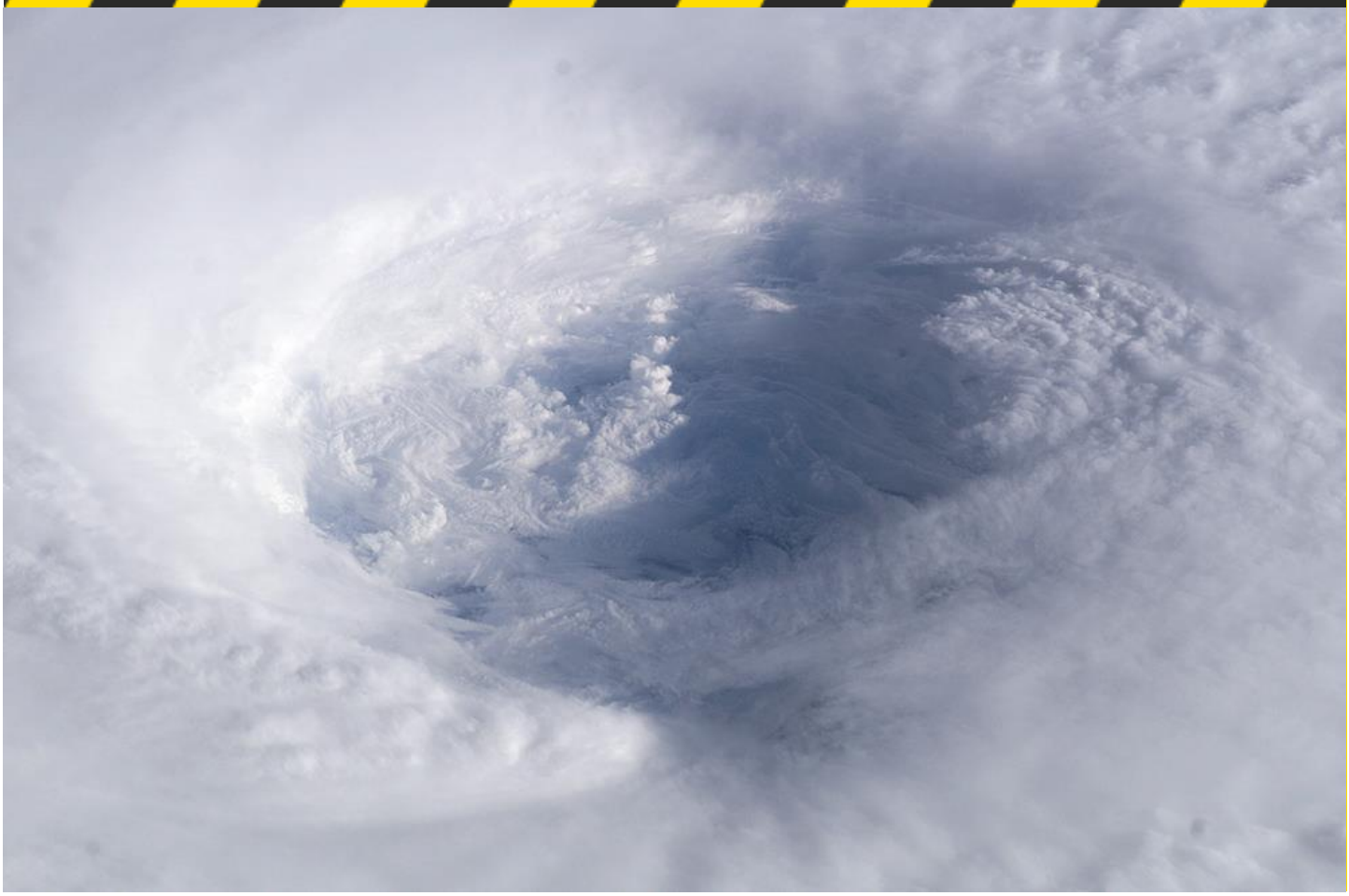

Version	Release history	Date
1.0	Initial release of document	04/09/2017

Publisher:
Bushfire and Natural Hazards CRC

September 2017

Citation: Kepert, J. D. (2017) Secondary eyewall formation in tropical cyclones. In M. Rumsewicz (Ed.) *Research forum 2017: proceedings from the research forum at the Bushfire and Natural Hazards CRC & AFAC Conference*. Melbourne: Bushfire and Natural Hazards CRC.

Cover: The eye of Hurricane Isabel, as seen from the International Space Station

TABLE OF CONTENTS

ABSTRACT

ABSTRACT TITLE

Jeffrey D. Kepert, Bureau of Meteorology and Bushfire and Natural Hazards CRC

Roughly half of all intense tropical cyclones experience an eyewall replacement cycle. In these events, a new eyewall forms concentrically around the original one. This secondary eyewall develops its own wind maximum, and both the secondary eye and the wind maximum typically intensify and contract, whilst the original eyewall and wind maximum weaken and eventually dissipate. While the evolution of a storm with concentric eyewalls is reasonably well understood, the mechanism or mechanisms by which the outer eyewall forms remain elusive. Understanding secondary eyewall formation is an important problem, for the subsequent eyewall replacement cycle can significantly affect the intensity of the storm, and the formation process and replacement cycle are usually associated with a major expansion of the outer wind field. Both these factors significantly affect the cyclone's impact.

We investigate a high resolution simulation of an eyewall replacement cycle. Boundary layer convergence due to friction substantially influences the evolution of the convection, and we present evidence for a positive feedback involving convection, vorticity and frictional convergence that governs the subsequent evolution of the system. In this feedback, frictional convergence strengthens the convection, stretching of vortex tubes in the buoyant updrafts increases the vorticity, and the vorticity structure of the storm determines the strength and location of the frictional updraft.

Changes in the structure and intensity of tropical cyclones cause difficulties for their management, especially if these changes occur in the last day or two before landfall. Our improved knowledge of these processes will lead to better forecasts and mitigation.

INTRODUCTION

In literature, "the eye of the storm" is an apt description for a region of peace and calm, around which tumult and turmoil reign (White, 1973). The analogy is to a tropical cyclone, where the eye, characterised by light winds, little cloud and little or no precipitation, is surrounded by the towering clouds of the eyewall. These eyewall clouds slope outwards from the centre of the storm with height, giving the appearance of a giant amphitheatre. The strongest winds are close to the surface immediately below these clouds, and they generate substantial amounts of rain. Often, the formation of a symmetric eye signifies that the cyclone is entering an intense and destructive phase. Truly, the literary analogy is apt.

About half of all intense tropical cyclones experience an eyewall replacement cycle (ERC). In an ERC, a secondary eyewall forms, concentric about the existing eyewall. Over the next day or so, the new eyewall intensifies and contracts, while the initial eyewall weakens and eventually disappears. During eyewall replacement, the cyclone's intensity is steady or weakens, but intensification typically resumes once the replacement of the initial eyewall is complete. Notable examples of Australian tropical cyclones with an ERC include cyclones Vance (1999), Larry (2006) and Yasi (2011).

Figure 1 illustrates a typical sequence, using satellite images from a variety of passive microwave sensors in the 85 – 91 GHz band on polar-orbiting satellites. These frequencies can see through the dense cirrus overcast that normally obscures our view of the inner workings of tropical cyclones, and hence reveal the rainband and eyewall structure. At the start of the sequence, the primary eyewall is the red circle near the centre, surrounded by the deep convection of the spiral rainbands. Over the next 12 hours, the rainbands become more symmetric and organise into an outer eyewall by 22:43 on 22 August (panel d). The outer eyewall continues to become more symmetric, while the inner one weakens and decays, with the last vestige visible at 12:47 on 28 August (panel i).

The fundamental dynamics of the tropical cyclone eyewall replacement cycle (ERC), after the outer eyewall has formed, have been understood for over three decades (Shapiro and Willoughby 1982; Willoughby et al. 1982). In contrast, the cause of the initial formation of the outer eyewall has proved to be more elusive. Numerous theories have been proposed (see the reviews by Rozoff et al. 2012; Wu et al. 2012) but a consensus has not been achieved. More recently, attention has focussed on the possible role of the boundary layer in secondary eyewall formation (SEF) (Huang et al. 2012; Kepert 2013; Abarca and Montgomery 2013). Therefore, it is of interest to diagnose the boundary-layer processes occurring during SEF and the subsequent evolution of the eyewalls. This report describes our analysis of a SEF/ERC simulated by a high-resolution WRF simulation of a hurricane. An earlier report (Kepert and Nolan 2014) focussed on the boundary layer dynamics. Here we consider the effects of heating and the cloud processes also.

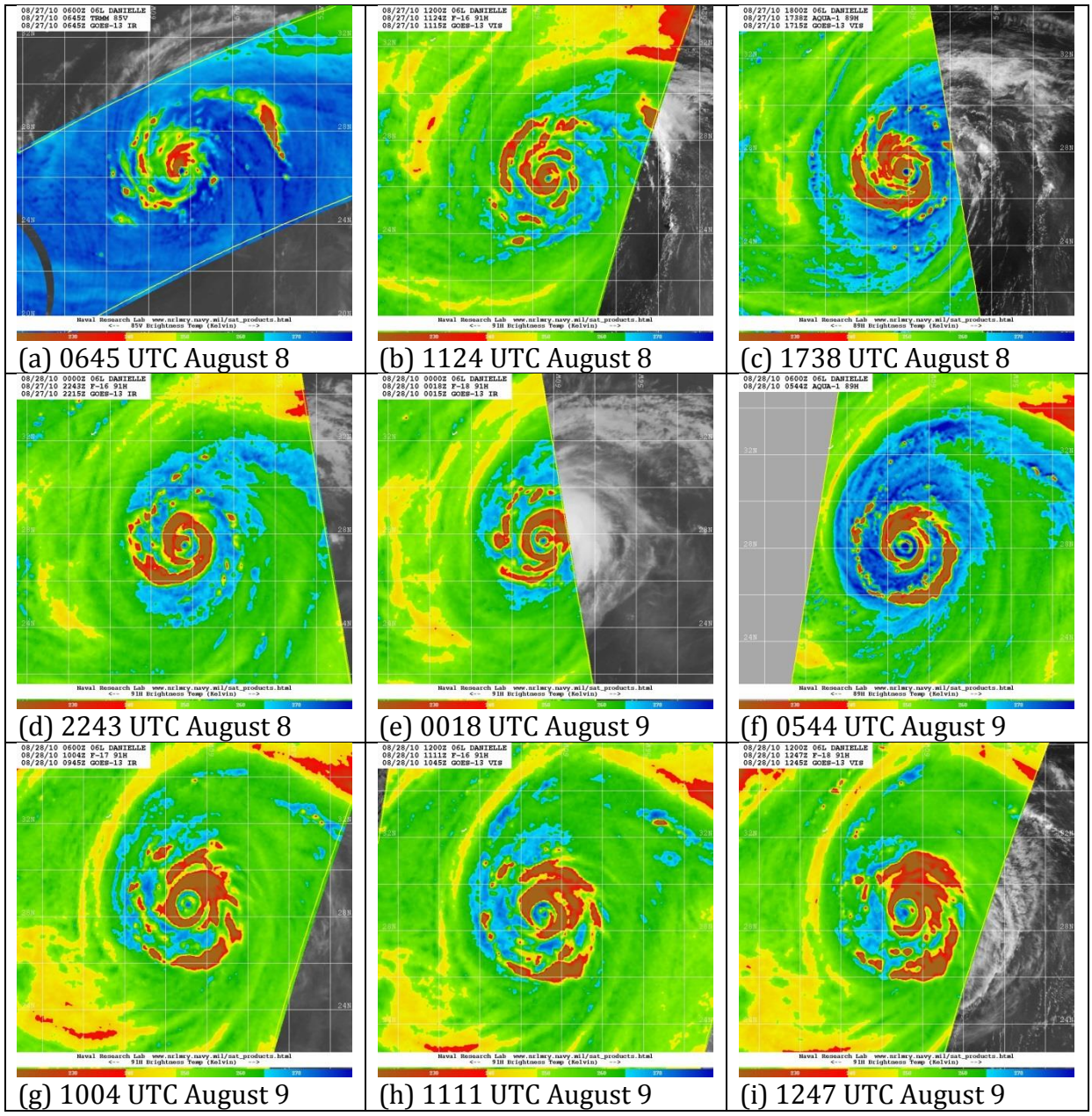

FIGURE 1: PASSIVE MICROWAVE IMAGERY IN THE 85 – 91 GHZ BAND FROM TRMM, DMSP AND AQUA SATELLITES, FOR HURRICANE DANIELLE OF 2010. RED AND BROWN SHADING INDICATE DEEP CONVECTION. TIMES AND DATES ARE INDICATED BENEATH EACH IMAGE. NOTE THAT THE TIME INTERVAL BETWEEN IMAGES VARIES. DATA COURTESY OF THE US NAVAL RESEARCH LABORATORIES.

THE SIMULATION

We use a WRF simulation of a TC that includes a SEF and ERC, prepared as a nature run for data assimilation experiments and described by Nolan et al. (2013). That simulation nested the WRF model (Skamarock et al 2008) from 27km down to 1 km and covered the full life of the hurricane, although we will focus attention on the 48-h period beginning at 0000 UTC 3 August. Details of the simulation, including the choice of the nesting and initial fields, and the model setup including the physical parameterizations, are given by Nolan et al. (2013).

Figure 2 shows the evolution of relevant fields, azimuthally averaged, from the simulation. Panel (a) shows the latent heat release, which is an indication of the occurrence of deep convection. The initial contraction and intensification of the primary eyewall is apparent, as is the formation and subsequent contraction and intensification of the secondary eyewall, indicated by the magenta curve. Panel (b) shows the similar evolution of the near-surface gradient wind, with the formation of the primary wind maximum and its replacement by the secondary one readily apparent. Note also the general outwards expansion of the wind field during the process. Panels (c) and (d) show the convective available potential energy (CAPE), a measure of the favourability of the atmosphere for convective cloud formation, and the vorticity[1] of the gradient wind, respectively, and will be discussed later, as will the green curve.

[1] In an axisymmetric vortex, the *vorticity* is defined as $\zeta = v/r + \partial v/\partial r$, where v is the azimuthal wind and r is radius. More generally, it is defined as the vector curl of the wind velocity. Given the crucial importance of vorticity to understanding these processes, it is appropriate to give a physical interpretation. Imagine a paddle wheel suspended in the air, with its axis vertical, moving with the wind. It may rotate, for instance if the flow is curved (curvature vorticity), or if the wind is stronger on one side of the paddle wheel than the other (shear vorticity). If observed from a fixed coordinate system, rather than the earth, it also rotates because the earth is rotating (planetary vorticity, accounted for by the Coriolis parameter f), and the *absolute vorticity* is the sum of the earth-relative and planetary vorticities. In tropical cyclones, the curvature and shear vorticity are of opposite sign outside of the eyewall, and these two terms cancel to some degree, but the net vorticity is mostly of the same sign as f; that is, cyclonic.

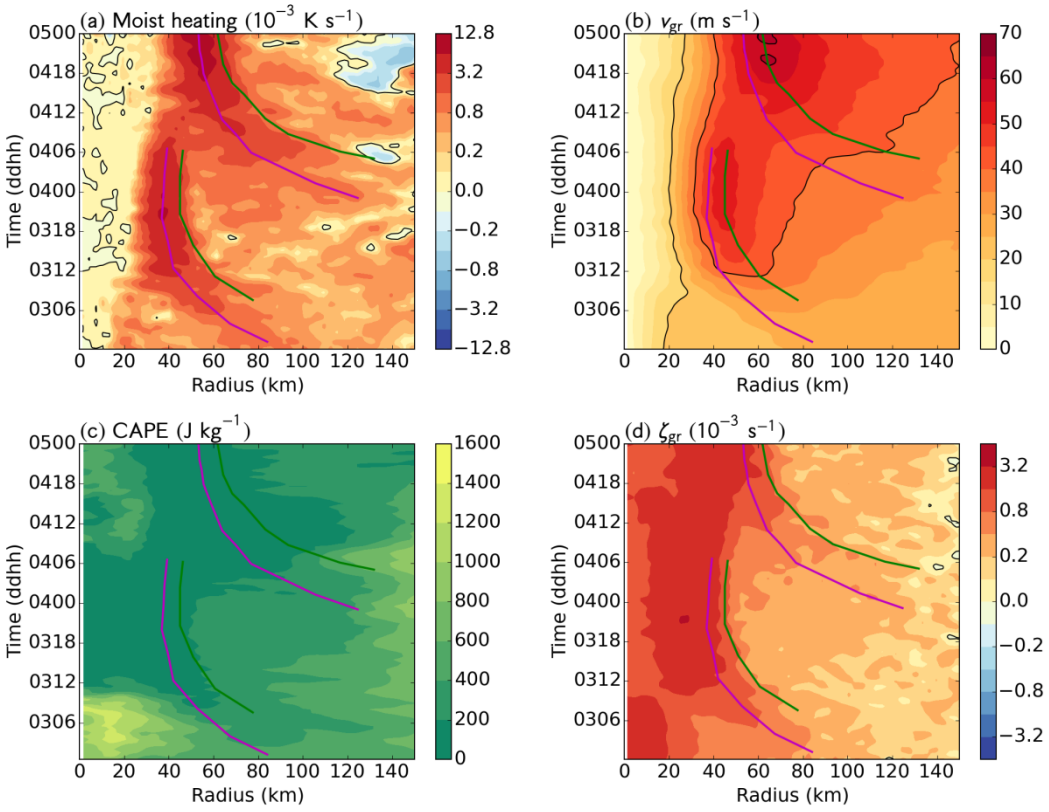

FIGURE 2: TIME-RADIUS DIAGRAMS OF (A) THE MOIST HEATING RATE, AVERAGED OVER 1-5 KM HEIGHT; (B) THE GRADIENT WIND SPEED AT 2-KM HEIGHT; (C) THE SURFACE-BASED CAPE; AND (D) THE VORTICITY OF THE GRADIENT WIND. ALL FIELDS ARE AZIMUTHALLY AVERAGED. THE MAGENTA CURVES INDICATES THE APPROXIMATE LOCATION OF THE TWO EYEWALLS, AS DETERMINED FROM THE MOIST HEATING. THE GREEN CURVES INDICATE THE APPROXIMATE LOCATION OF THE RADII OF MAXIMUM NEGATIVE RADIAL VORTICITY GRADIENT.

ANALYSIS TOOLS

The tropical cyclone flow can be divided into two components: the primary circulation, which is the rotational flow, and the secondary circulation, which consists of inflow mainly near the earth's surface, ascent mainly near the cyclone centre, and outflow mainly in the upper troposphere. The secondary circulation is often described as "in, up and out". It is forced by two main mechanisms: surface friction causing the near-surface flow to spiral inwards rather than being purely circular, and latent heat release in the clouds, particularly in and around the eyewall, which causes buoyant ascent. Mathematically, we adopt the convention that a radial flow component directed towards the centre of the storm (i.e. inflow) has a negative sign, whereas outflow is positive.

The frictional component of the secondary circulation, to a first order approximation, does not intensify the cyclone or change its structure, because the inwards advection of absolute angular momentum[2] nearly balances its destruction by surface friction (Kepert 2013). The heating component, in contrast, can intensify the cyclone since its lower branch advects absolute angular momentum inwards, spinning up the storm by the "ice-skater effect".

We assess the heating-induced component by the Sawyer-Eliassen equation, and the frictional component using a diagnostic boundary-layer model.

THE SAWYER-ELIASSEN EQUATION

The Sawyer-Eliassen equation (SEeq) diagnoses the secondary circulation due to latent heat release and other diabatic heating sources. It can also diagnose the effect of momentum sources and sinks, but may be less accurate for boundary layer friction due to the violation of a key assumption within the boundary layer.

We use the form of the SEeq given by Pendergrass and Willoughby (2009), discretised on a uniform grid with 75 grid points in radius, from 4 to 300 km, and 39 in height, from 0 to 19.5 km. The boundary conditions are that the flow perpendicular to the inner, upper and lower boundaries is zero, and that the flow is purely horizontal at r = 300 km. The discretised equation is solved directly using QR decomposition, which is feasible on modern computers with a problem of this size. Although not especially efficient, direct solution avoids the problem of potential nonconvergence of iterative methods should the SEeq be slightly non-elliptic, as sometimes happens in the upper-level outflow at large radius.

In this application, the inputs to the SE equation describing the structure of the storm and the heating are taken to be the azimuthal means, calculated

[2] Absolute angular momentum is similar to the familiar concept of angular momentum, but is calculated from a fixed frame of reference and therefore takes into account the earth's rotation. If r is the radius and v the azimuthal wind, then the absolute angular momentum is Ma = rv + 0.5fr2, where the Coriolis parameter f is the local vertical component of the earth's rotation.

directly from the WRF simulation output. Heating is taken to be the sum of latent heat exchanges and radiation.

THE BOUNDARY-LAYER DIAGNOSTIC MODEL

The boundary-layer diagnostic model has been described by Kepert and Wang (2001), and Kepert (2012, 2017). It solves the equations of fluid motion, with high-quality parameterisations of friction and turbulence, for a prescribed fixed pressure field representative of a tropical cyclone. It is run forward in time to a steady state, and the resulting flow represents the equilibrium boundary-layer flow given that pressure forcing. One day of model time usually gives a sufficiently steady state. For convenience, the pressure field is specified in terms of the gradient wind,

$$\frac{v^2}{r} + fv = -\frac{1}{\rho}\frac{\partial p}{\partial r},$$

where v is the azimuthal wind, r is radius, f is the Coriolis parameter, ρ is density and p is pressure.

In contrast to the SEeq, where the domain includes the full depth of the troposphere, here the domain is only 2.25 km deep, sufficient to contain the boundary layer.

As with the SE equation, the necessary input to this model of the gradient wind is calculated from the azimuthal mean of the WRF simulation output, at hourly intervals. The boundary-layer models turbulence and friction parameterisations were configured to be reasonably consistent with those in WRF.

The boundary-layer model has been shown to be able to accurately reproduce the distribution of vertical motion in tropical cyclones when used in this way (Kepert and Nolan 2014, Zhang et al 2017).

DYNAMICS OF THE EYEWALL REPLACEMENT CYCLE

DOES FRICTIONAL CONVERGENCE INFLUENCE THE CONVECTION?

Figure 3a shows the azimuthal-mean vertical velocity at 1-km height from the WRF simulation. The evolution of the two eyewalls is clear, and closely follows that of the latent heat release in Figure 2a, as is usual in tropical cyclones. Figure 3b shows the diagnosed frictional updraft from the boundary-layer model, which clearly reflects a very similar pattern. There are two significant differences: the updraft in the boundary-layer model is consistently weaker, and located at slightly larger radius. We will show shortly that the difference in strength of the updraft is due to the absence of buoyant convection in the boundary-layer model.

To confirm that boundary-layer frictional convergence is the cause of the convection, we have to eliminate other possible causes, in particular thermodynamic factors. Convective available potential energy (CAPE), shown in Figure 2c, is a widely-used measure of the favourability of the atmosphere for convection, with higher numbers being more favourable. The values shown there are somewhat, but not strongly, favourable. There are no features in the CAPE field which would promote convection at the time and location of the secondary eyewall. Indeed, the CAPE at this time is amongst the lowest in the figure, and decreases as the eyewall strengthens. This decrease is due to two reasons (not shown): cold downdrafts from convection cooling and drying the lower troposphere, and the broadening of the upper warm core reducing the equilibrium level for deep convection.

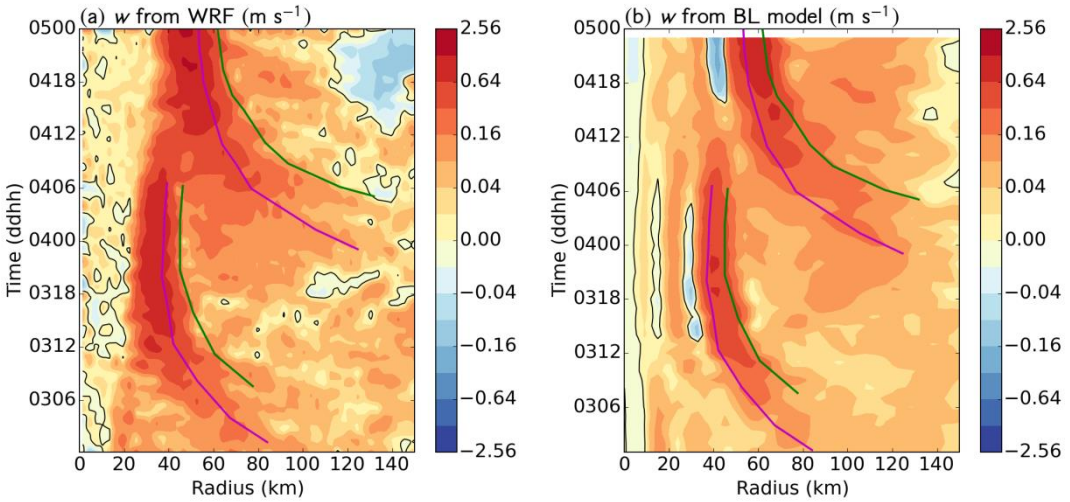

FIGURE 3: TIME-RADIUS PLOTS OF THE AZIMUTHAL-MEAN VERTICAL VELOCITY AT 1-KM HEIGHT, FROM (A) THE WRF SIMULATION AND (B) THE DIAGNOSTIC BOUNDARY-LAYER MODEL.

HOW DOES THE CONVECTION ALTER THE CYCLONE STRUCTURE AND INTENSITY?

The modelled secondary circulation at four key times before and during the ERC are shown in Figure 4, together with the corresponding diagnosed fields from a preliminary calculation with the SEeq. There is generally quite good agreement. One systematic differences is that the diagnosed main updrafts are often too weak in the lowest 2 km of the atmosphere, likely due to the absence of friction in this calculation. Indeed, the updraft in this region appears to be forced by both latent heat release and friction, since both diagnostic methods underestimate it. The diagnostic calculation also has inflow around 3 km height and 80 km radius, whereas WRF has outflow. Again, this may be due to the absence of friction. There are also a number of technical issues still to be resolved with the SEeq calculation, whose contribution is presently unknown – we note that this is a preliminary calculation.

Nevertheless, there is quite good agreement with the WRF simulation. We may therefore appeal to earlier studies with the SEeq (Shapiro and Willoughby 1982, Willoughby et al 1982) to note that the expected storm evolution from this pattern would be for the outer wind maximum to intensify and contract, qualitatively consistent with the evolution in Figure 2b. Future work will examine the extent to which quantitative agreement is obtained.

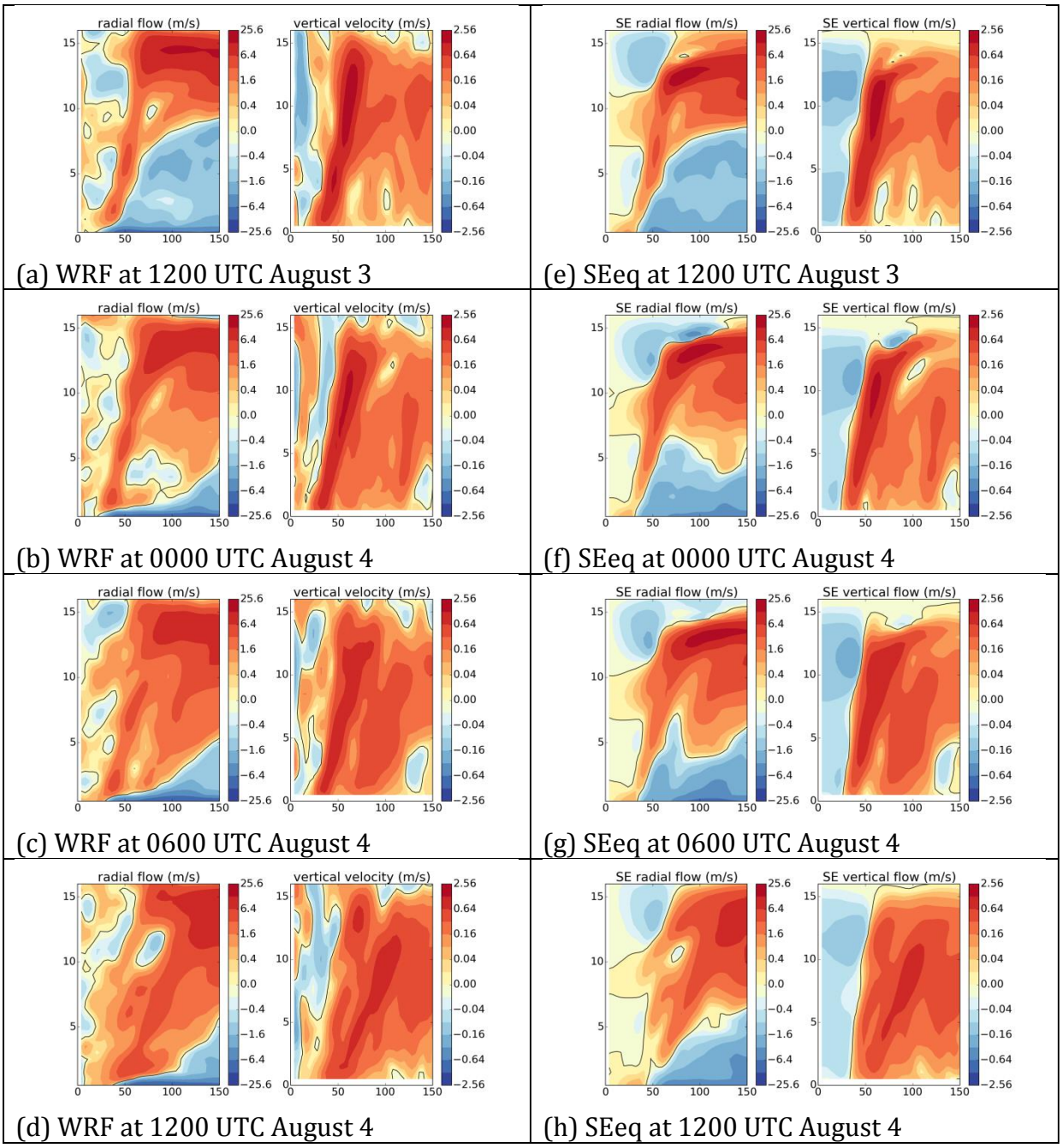

FIGURE 4: SECONDARY CIRCULATION DURING THE ERC AND SEF. PANELS (A – D) SHOW THE AZIMUTHAL-MEAN RADIAL WIND (LEFT, POSITIVE IS OUTWARDS) AND VERTICAL WIND (RIGHT, POSITIVE IS UPWARDS) FROM THE WRF SIMULATION AT TIMES AS INDICATED. PANELS (E – H) SHOW THE CORRESPONDING DIAGNOSED SECONDARY CIRCULATION USING THE SEEQ.

HOW DOES THE CYCLONE'S PRESSURE FIELD AFFECT THE FRICTIONAL CONVERGENCE?

We have seen above that the diagnosed frictional convergence determines the location and intensity of the convective heating. The only data passed from WRF to the diagnostic model in this calculation is the pressure field, in the form of the gradient wind. The question, then, is what characteristic of the pressure field leads to localised updrafts outside of the primary eyewall?

In Figure 3, we saw that the diagnostic BL model reproduces the location and relative strength of the two eyewall updrafts reasonably accurately, although underpredicts the strength because in the WRF simulation that is enhanced by the additional forcing from buoyant convection. It is also apparent in this figure that the changes in the gradient wind are spatially smoother than the vertical velocity response, and are relatively subtle. Pressure is the radial integral of gradient wind, so the changes in pressure must be even smoother than for gradient wind[3]. Nevertheless, these subtle changes must be responsible for the changes in the frictional forcing of the updraft, because they are the only information passed to the boundary-layer model. In other words, we know **that** the pressure field affects the frictional convergence, and we need to determine **how**.

Kepert (2001) developed a simplified diagnostic tropical cyclone boundary layer model. Compared to the model used here, the simplifications included a linearization, and adoption of less realistic representations of turbulent diffusion and the air-sea momentum transfer. While calculations with this model are expected to be less accurate than from the full diagnostic model, they offer the great benefit that an analytic solution is available. That is, we can directly examine the equations to understand how the vertical velocity relates to the pressure (or gradient wind) structure.

Kepert (2013) used that model to show that near the eyewall(s) of typical tropical cyclones, the updraft is approximately proportional to the radial gradient of the vorticity of the gradient wind, multiplied by the drag the wind exerts on the sea surface (approximately proportional to the square of the wind speed), divided by the square of the absolute vorticity. This equation suggests that we can expect to find enhanced updrafts where there is a locally strong negative radial vorticity gradient. Such gradients are especially effective if they occur where the vorticity is relatively low, because of the division by the square of the vorticity. The surface friction has a lesser effect on locating the updraft, because it varies relatively slowly with radius.

[3] Differentiation acts as a high-pass filter, emphasising the small scales, as can be easily shown using the Fourier transform.

DISCUSSION AND CONCLUSIONS

Figure 2b,d and Figure 3a compare the joint evolution of the vorticity of the gradient wind, the frictional updraft, and the moist heating. These figures show the mutual contraction of the region of strong vorticity gradient and the region of strong convective latent heat release. Indeed, a similar relationship is also apparent earlier in the cyclone's life, during the initial contraction and intensification of the primary eyewall between 0000UTC and 1200UTC on August 3.

Clearly, these features are strongly correlated. However, correlation is not causation. The fact that A and B are correlated may occur for several reasons: A causes B, B causes A, or that both are caused by some third factor C.

In this paper, we have provided additional information that does allow us to attribute cause. In particular, using the diagnosed frictional convergence, which depends only on the cyclone's pressure field, we have shown that the distribution of vertical velocity at the top of the boundary layer is determined largely by frictional processes, although friction is insufficient to explain the full magnitude of the ascent. By comparing the evolution of the diagnosed frictional convergence to that of the convective latent heat release, together with the absence of any features sufficient to explain the localisation of the convection in the stability or moisture fields, we show that the frictional updraft is largely determining the location and strength of the convection. Calculating that part of the secondary circulation induced by heating, using the Sawyer-Eliassen equation largely accounts for that part of the low-level updraft missing from the frictional calculation. The evolution of the vortex structure explained by advection of absolute angular momentum by this secondary circulation is largely consistent with the evolution of the cyclone; that is, it leads to changes in the gradient wind that are similar to those in the WRF simulation. Most importantly, these include an inwards migration and strengthening of the vorticity features that we have theoretically linked to the evolving frictional updraft.

To summarise, we have confirmed that the positive feedback mechanism hypothesised by Kepert (2013) and further discussed by Kepert and Nolan (2014) and Kepert (2017) is indeed operating in this case. Here, vorticity-induced boundary-layer convergence acts to promote convection, provided that the stability and moisture are also favourable. Vortex-stretching in convective updrafts increases the local vorticity. We have analysed the combined, cyclone-scale, effect of many individual clouds by applying their combined heating to the Sawyer-Eliassen equation, but analyses at the cloud scale (not shown) similarly show that convective updrafts are acting to increase the vorticity beneath the developing secondary eyewall. These vorticity changes in turn further strengthen the frictional updraft. There is a further important subtlety in all of this, in that the relative location of the various processes is important for the precise details of the interaction, particularly the initial rapid contraction of the outer eyewall, followed later by slower contraction and intensification. These can be largely explained as a contribution of nonlinearity in the boundary layer, as detailed in Kepert (2017).

PRACTICAL IMPLICATIONS

Forecasting ERCs is challenging, because it is clear from the work described here that the changes in the early stages are quite subtle, and therefore difficult to detect. This is especially true in the harsh environment of tropical cyclones, where observations are difficult to take. Modelling ERCs is likewise challenging, for this work implies that the interaction between friction, clouds and pressure in the cyclone must be represented with sufficient fidelity. Nevertheless, the success of the simulation used here and others shows that that fidelity has been achieved in current NWP systems.

The initialisation of such simulations is challenging, especially since the early signs of an ERC are subtle. Small errors in the initial pressure field could completely remove local vorticity perturbation, and hence the frictional updraft, or add a spurious one. The necessary precision in the initialisation will be beyond the reach of our observing and data assimilation systems, at least in the absence of aircraft reconnaissance, for some time. Ensemble prediction methods provide the only presently viable means of dealing with this uncertainty.

In spite of these considerable difficulties, forecasting ERCs is important. They represent a substantial additional difficulty for intensity forecasting, because of their large impact on the intensity evolution of the storm. They also strongly affect the ocean response. A substantial import of vorticity to the storm in the region of the developing outer eyewall seems to be an inherent part of the ERC process, and this import of vorticity explains (through Stoke's theorem) the wind field expansion. The wind field expansion affects not just the width of the damage swath, but also the timing and duration of damaging winds. It also profoundly increases the ocean hazard, because applying strong winds to a larger area of the ocean's surface greatly increases the severity and extent of storm surge, damaging waves and coastal erosion. With the high concentration of vulnerable populations and infrastructure near the coast in Australia, improving our ability to predict ERC will clearly help mitigate tropical cyclone impacts.

REFERENCES

Kepert, J. D., 2001: The dynamics of boundary layer jets within the tropical cyclone core. Part I: Linear theory. *J. Atmos. Sci*., **58**, 2469–2484, doi:10.1175/1520-469(2001)058,2469:TDOBLJ.2.0.CO;2.

Kepert, J.D., 2013: How does the boundary layer contribute to eyewall replacement cycles in axisymmetric tropical cyclones? *J. Atmos. Sci*., **70**, 2808–2830, doi:10.1175/JAS-D-13-046.1.

Kepert, J.D., 2017: Time and space scales in the tropical cyclone boundary layer, and the location of the eyewall updraft. Submitted to *J. Atmos. Sci.*

Kepert, J.D. and D.S. Nolan, 2014: Reply to ''Comments on 'How Does the Boundary Layer Contribute to Eyewall Replacement Cycles in Axisymmetric Tropical Cyclones?''' *J. Atmos. Sci*., **71**, 4692-4704, DOI: 10.1175/JAS-D-14-0014.1

Kepert, J.D., and Y. Wang, 2001: The dynamics of boundary layer jets within the tropical cyclone core. Part II: Nonlinear enhancement. *J. Atmos. Sci*., **58**, 2485–2501, doi:10.1175/1520- 469(2001)058,2485:TDOBLJ.2.0.CO;2.

Nolan. D.S., R. Atlas, K. T. Bhatia, and L. R. Bucci, 2013: Development and validation of a hurricane nature run using the joint OSSE nature run and the WRF model. *J. Adv. Model. Earth Syst*., **5**, 382–405, doi:10.1002/jame.20031.

Pendergrass, A. G., and H. E. Willoughby, 2009: Diabatically induced secondary flows in tropical cyclones. Part I: Quasisteady forcing. *Mon. Wea. Rev*., **137**, 805–821.

Shapiro, L. J. and H. E. Willoughby, 1982: The response of balanced hurricanes to local sources of heat and momentum. *J. Atmos. Sci*., **39**, 378–394.

Skamarock, W. C., J. B. Klemp, J. Dudhia, D. O. Gill, D. M. Barker, M. G. Duda, X.-Y. Huang, W. Wang, and J. G. Powers (2008), A description of the advanced research WRF version 3, NCAR Tech. Note, 4751STR, Boulder, Colorado, pp. 113.

White, P.V.M., 1973: *The Eye of the Storm.* Jonathan Cape, 608pp.

Willoughby, H. E., J. A. Clos, and M. G. Shoreibah, 1982: Concentric eyewalls, secondary wind maxima, and the evolution of the hurricane vortex. *J. Atmos. Sci*., **39**, 395–411.